MIT Open Access Articles

Resistive and Capacitive #-Ray Dosimeters Based On Triggered Depolymerization in Carbon Nanotube Composites

Massachusetts Institute of Technology

Resistive and Capacitive γ-Ray Dosimeters Based On Triggered Depolymerization in Carbon Nanotube Composites

Lukas Zeininger[†], **Maggie He**[†], **Stephen T. Hobson**[‡,#], and **Timothy M. Swager**[†]

[†]Department of Chemistry, Massachusetts Institute of Technology, Cambridge, Massachusetts 02139, United States

[‡]Seacoast Science Inc., Carlsbad, California 92011, United States

Abstract

We report γ-ray dosimeters using carbon nanotubes wrapped with metastable poly(olefin sulfone)s (POSs) that readily depolymerize when exposed to ionizing radiation. New POSs, designed for wrapping single-walled carbon nanotubes (SWCNTs), are synthesized and characterized. The resulting POS-SWCNT composites serve as the active transducer in a novel class of γ-ray dosimeters. In our devices, polymer degradation results in immediate changes in the electronic potential of the POS-SWCNT active layers by decreasing the electron tunneling barriers between individualized tubes and by creating enhanced cofacial π–π electron contacts. By incorporating the SWCNT-POS composites into small resistive device platforms, we establish a rare example of real-time detection and dosimetry of radioactive ionizing radiation using organic-based materials. We show that the sensitivity of our platform closely depends on the intrinsic stability of the polymer matrix, the opacity toward γ-rays, and the dispersion efficiency (i.e., the individualization and isolation of the individual SWCNT charge carriers). Resistance decreases up to 65% after irradiation with a 40 krad dose demonstrates the high sensitivity of this novel class of γ-ray sensors. In addition, the detection mechanism was evaluated using a commercial capacitive device platform. The ease of fabrication and low power consumption of these small and inexpensive sensor platforms combined with appealing sensitivity parameters establishes the potential of the poly(olefin sulfone)-SWCNT composites to serve as a new transduction material in γ-ray sensor applications.

Keywords

carbon nanotubes; degradable polymers; poly(olefin sulfone)s; radiation sensor; γ-radiation

Gamma (γ) ray sensors capable of reliably, sensitively, and quantitatively converting an adsorption of radioactive ionizing radiation into a measurable (physical) signal represent a

The authors declare the following competing financial interest(s): We will be filing a patent on this method and materials.

crucial technology in many fields including medical radiation therapy, applied physics, industrial imaging, food and medical sterilization, and nuclear security.(1) When designing a γ-ray sensor, the key properties of consideration are the determination of a durable and reliable transduction material that (i) exhibits good sensitivity for γ-rays, (ii) demonstrates environmental stability over the desired device lifetime without premature degradation, (iii) meets the requirements of the chosen application, such as a potential to operate at room temperature, (iv) can be produced with low synthetic/fabrication effort and operated with low maintenance cost, and (v) is ideally capable of creating a real-time signal. Many different technologies have been investigated as γ-ray dosimeters. Among them, ionization chambers are the most important dosimeters to date, as a result of their sensitivity and relatively flat energy response. However, their applications are limited because of their large size and high bias voltage requirements for achieving acceptable ionization collection efficiencies. Similarly, other technologies, such as silicon diodes, metal-oxide semiconductor field effect transistors (MOSFETs), thermo-luminescent dosimeters (TLDs), and optically stimulated luminescence dosimeters (OSLDs), are often cumbersome and/or costly to use and fabricate, require an operation at low temperatures, or are unable to create a real-time signal.(2,3)

Molecular and nanoscale material-based radiation sensors can exhibit unique properties to overcome these obstacles.(4) Radiation sensors utilizing small molecules, polymers, and inorganic or organic nanoparticles have been shown to enable simple, yet robust systems for monitoring and quantifying ionizing radiation. To this end, the excellent charge transport and ionization collection properties of carbon nanotubes (CNTs) have been efficiently utilized to miniaturize ionization chambers and lower bias voltages.(5,6) Other nanoparticle-based systems monitor photoluminescence from semiconductor quantum dots or plasmonic nanoparticle enhancements of surface enhanced Raman scattering. Small molecule based radiation sensor systems include the degradation of fluorescent molecules as a result of high-energy irradiation as a "turn-off" sensor, as well as aggregation-induced emission "turn-on" sensors for silole compounds.(7,8) The formation or degradation of polymers triggered via free radicals generated by high energy radiation has emerged as a very appealing method. In contrast to the nanoparticle detection schemes outlined above, polymer-based systems are attractive as a single chemical trigger can initiate a chain reaction. Thus, chemistry induced by a single high energy particle can be amplified to generate a large signal.(9)

Polymeric materials that rapidly depolymerize into volatile components on command are attractive for many applications, including packaging, encapsulation, drug delivery, transient electronics, and sensor applications.(10–12) Examples for these types of self-immolating polymers include low-ceiling temperature polyaldehydes, polyglyoxylates, metallo-supramolecular polymers, and poly(olefin sulfone)s (POSs).(13–17) POSs exhibit low ceiling temperatures and have been shown to undergo triggered depolymerization when exposed to heat,(18) base,(19,20) or ionizing radiation.(21,22) POSs possess main chain sulfonyl (SO_2) groups and can be easily synthesized by low temperature free radical polymerization of olefin monomers in liquefied sulfur dioxide. As a result of their characteristics, POSs have been targeted for the development of photoresists and other degradable materials.(19) The generation of radicals, abstraction of acidic protons, or the

removal of an electron from the polymer backbone can lead to polymer chain scission, and therefore one triggering event can cause the whole polymer to decompose.

To translate POS materials to sensor applications, triggered depolymerization must create a measurable modification, amplification, or reduction of a detectable signal. Therefore, as is typical for chemical sensors, a sensory material that selectively responds to a target stimulus needs to be connected to an efficient physicochemical transducer to provide a readable, and ideally real-time, signal.(23) CNTs are exceptional transduction materials and have found utility in a variety of chemical sensor applications.(24) The lowest resistance for electrical charge transport is along the axis of the nanotube with higher resistivity inter-nanotube electronic couplings being necessary for bulk conduction. Two general transduction mechanisms dominate CNT transduction: (i) triggered modification of intra-CNT transport, where a binding event pins, liberates, creates, or destroys carriers in the nanotube or (ii) induced inter-CNT transport by adding, removing, or modifying isolating materials between nanotubes to change or eliminate electron tunneling barriers between CNTs. The latter is ideally matched to a triggered depolymerization of an isolating polymer matrix to increase the transport through a CNT nanowire network.(24,25) In the most straightforward manifestation, a network of CNTs is placed between two electrodes with a static potential bias (V) and the resulting output current (I) changes with the resistance (R) of the active layer according to Ohm's Law. In impedance or capacitive devices, measurable changes of the dielectric constant (ε) can potentially lead to increased sensitivity of the sensor device. (26,27) Advantages of CNT-based nanowire resistive sensors include straightforward signal detection, low power consumption, ease of miniaturization, and sensitivity, which combine to facilitate real-time detection. The introduction of new polymer matrices capable of programmed degradation upon high-energy irradiation, along with innovations in the fabrication of polymer-CNT composites offers an appealing strategy to enable real-time dosimetric electrical detection of γ-irradiation. Low cost CNT materials are readily integrated into small devices and have similar opacity to biological tissue, all of which are desirable for γ-ray dosimeters.

In this work, we introduce new single-walled carbon nanotube (SWCNT)—poly(olefin sulfone) (POS) composite materials that function as dosimeters for ionizing γ-rays. We have synthesized and characterized new POSs that have been optimized to exhibit strong binding interactions with pristine or functionalized SWCNTs. These efforts build on previous schemes from our group that made use of multiwalled carbon nanotubes.(28) Using our new designs, we have enhanced the sensitivity, demonstrated real-time detection, and evaluated capacitive transduction. The central concept of this platform (Scheme 1) is the isolation of SWCNTs in the insulating polymer matrix that undergoes rapid depolymerization when exposed to ionizing radiation. Disassembly of the polymer matrix results in increased contacts between the SWCNTs and increased conduction and capacitance. Small resistive and capacitive device platforms were used for real-time detection and dosimetry of ionizing radiation. In addition, we studied the influence on and correlation between the dispersion quality, the intrinsic polymer stability, and the γ-ray sensitivity of our devices. The latter is addressed by incorporating high atomic number bismuth molecular and nanoparticulate components in the polymer-SWCNT matrix.

Materials and Methods

Detailed experimental procedures are described in the Supporting Information. All chemicals were purchased from Sigma-Aldrich and were used as received, except for sulfur dioxide, which was purchased from Airgas. 6,5-Chirality enriched SWCNTs were acquired from Sigma-Aldrich. Unless stated otherwise, all reactions were performed under an oxygen-free atmosphere of argon. Graduated flasks were used for polymerization reactions with condensed sulfur dioxide. NMR spectra were obtained on a Bruker Avance (400 MHz). ATR-FTIR spectra were obtained using a Thermo Scientific Nicolet 6700 FTIR with a Ge crystal for ATR. Polymer molecular weights were determined at room temperature on a HP series 1100 GPC system in THF at 1.0 mL/min (0.5 mg/mL sample concentrations), approximate molecular weights were estimated using a polystyrene calibration standard. UV–vis-NIR absorption spectra were obtained using an Agilent Cary 5000 spectrophotometer. Raman spectra were collected using a Horiba LabRAM HR800 Raman spectrometer. X-ray photoelectron spectroscopy (XPS) was performed with a PHI Versaprobe II XPS spectrometer. A Gammacell irradiator "Gammacell 200" with a ^{60}Co source was used for γ-irradiation of both the resistive and capacitive devices. Typically, devices were irradiated for 10 min to achieve a radiation dose of approximately 50×10^3 rad.

Synthesis of Polymers

The general synthesis of poly(olefin sulfone)s has been reported previously and was carried out following literature procedures. In brief, a typical polymerization procedure was carried out as follows: Sulfur dioxide was condensed into a graduated vessel at −78 °C. After transferring the reaction vessel into a −45 °C acetone/dry ice bath, the olefin monomer(s) were added in the desired ratio and the solution was stirred for 15 min. Then, *tert*-butyl hydroperoxide (5–6 M in decane) was added to the solution. The polymerization was allowed to proceed at −45 °C for 2 h. The polymerization was stopped by pouring the reaction mixture into cold methanol. After reaching RT, the solvent was evaporated and the resulting powder was redissolved, reprecipitated, and washed three times before the polymer was dried under vacuum overnight. The synthesis of **POS 1**, **POS 2**, **POS 3**, and **POS 7** has been described previously and the characterization of these polymers was consistent with the previous reports.(18,20,22,28)

Preparation of POS-SWCNT Dispersions

To a solution of POS (10 mg) in *N,N*-dimethylformamide or water (5 mL), SWCNTs (1 mg) were added and the resulting mixture was sonicated for 1 h in an ultrasonic bath (Branson, 3510) chilled with ice and then allowed to reach room temperature. Subsequently, the suspension was centrifuged for 30 min at 15,000 rpm and allowed to stand overnight undisturbed. The isolated supernatant was directly used for the device fabrication via spray coating or dropcasting unless otherwise indicated. For UV–vis-NIR absorption spectroscopy, the isolated supernatant was further diluted.

Fabrication of Dosimetric Devices

For the preparation of resistive γ-ray sensor devices, glass slides (VWR Microscope Slides) were cleaned by sonication in acetone for 5 min followed by UV-ozone treatment using a

UVO cleaner (Jelight Company Inc., Model 42) for 20 min. A 10 nm layer of chromium (99.99%, R.D. Mathis) and a subsequent 100 nm layer of gold (99.99%, R.D. Mathis) were deposited through a custom stainless steel mask using a thermal evaporator (Angstrom Engineering). The gap between one pair of gold electrodes was 1.0 mm. The desired amount of POS-SWCNT dispersion was loaded into an airbrush (Revolution BR, Iwata) and manually spray-coated on the gap of gold electrode pairs through a homemade transparency film (CG3700, 3M) mask. In order to prevent unwanted nozzle drips and overwetting on the substrate surface, which resulted in nonuniform deposition of composites, the dispersion was sprayed intermittently multiple times with an injection rate of about 40 μL/min at a distance of 10 cm from the substrate placed on a 90 °C hot plate under N_2 carrier gas of 2 bar pressure. After the spraying process, the resulting substrate was thermally annealed at 90 °C for 2 h. The sheet resistance of POS-SWCNT composite films before, during, and after γ-irradiation was measured using a Keithley 2400 source meter or a Keithley 2000 multimeter. For a read-out of the capacitance change of POS-SWCNT composites upon γ-irradiation a SC-200 sensor chip platform provided by Seacoast Inc. was used. The sensor chips were coated via micropipetting the POS-SWCNT dispersions directly on top of the sensor chips. The capacitance change of POS-SWCNT composites deposited on Seacoast SC-200 sensor chips was recorded using the software SC-200 Series Data Logger.

Results and Discussion

Synthesis of Poly(olefin sulfone)s

Critical to the design of our sensor materials is the isolation of carbon nanotubes in a nonconductive polymeric matrix. In this work, we synthesized poly(olefin sulfone)s that were designed to effectively disperse, debundle, and individualize SWCNTs. Standard synthetic conditions involve bulk polymerization at low temperatures (–45 °C) with sulfur dioxide serving as both solvent and comonomer and *tert*-butyl hydroperoxide as the initiator. The polymerization reaction proceeds in a strictly alternating fashion as a result of the preferred reaction of sulfonyl radical chain ends with the electron rich olefin monomer(s) in SO_2. The resulting poly(olefin sulfone)s **POSs 1**–**10** are shown in Figure 1.

In addition to new materials, previously reported **POSs 1** and **2** were synthesized using 1-hexene and cyclohexene as olefin monomers. To enhance the dispersibility of SWCNTs, we synthesized **POS 3**, which possesses a benzoate substituent, which visibly increases the SWCNT dispersibility in DMF presumably as a result of π–π-stacking with the CNT sidewalls. Moreover, **POS 3** has a lower decomposition temperature ($T_{decomp} = 188$ °C) indicating that it is more susceptible to degradation as compared to **POSs 1** and **2**.

We also targeted the Lewis basic **POS 4** based on the previously observed fact that poly(4-vinylpyridine) (P4VP) creates exceptionally stable SWCNT dispersions presumably as a result of interactions between the nitrogen lone pairs and the SWCNT sidewalls.(29) Additionally, aromatic N-heterocycles can display π–π-stacking interactions with CNTs and be functionalized with ions for the creation of expanded materials diversity.(29,30) Unfortunately, the random copolymerization of SO_2 with 4-vinylpyridine or 1-allylimidazole failed, most likely due to the basicity of these monomers and the base-sensitivity of the polymer backbone.(30) However, we were able to incorporate this functionality in a ter-

polymerization scheme involving an excess of 1-hexene as comonomer, yielding poly(1-hexene sulfone)-*co*-(1-allylimidazole sulfone) (**POS 4**) with an x/y ratio of 1.0/9.8 in moderate yields of 78%. The addition of 1-hexene as a comonomer successfully stabilized the polymer up to T_{decomp} = 148 °C.

As alternative polymer matrices, we explored the synthesis of new amphiphilic **POSs 5** and **6**. In an alternative wrapping mechanism, these polymers were designed to stabilize SWCNTs in polar solvents. In amphiphilic polymer-CNT dispersions Coulombic attractions between the polar polymer side chains and solvent as well as the hydrophobic and van der Waals interactions between the polymer surfactant tails and CNT surfaces work synergistically to stabilize the solution. Amphiphilic **POS 5** was produced by ter-polymerization of 1-hexene, di(ethylene glycol) vinyl ether, and SO_2 in 59% yield. A second amphiphilic ionic surfactant polymer, **POS 6**, poly(1-hexene sulfone)-*co*-(sodium 4-vinylbenzenesulfonate sulfone), was also synthesized with yields of 75%. The successful and simple generation of these **POSs 5** and **6** illustrates the facile generation of designer radiation sensitive copolymers. In order to compare these newly synthesized polymers to our previous studies,(28) **POS 7** was synthesized. The synthesis of **POS 7** involved multiple steps and incorporates a pyrene moiety to bind to the surfaces of SWCNTs, and a high-atomic-number bismuth complex component to increase γ-ray opacity.

The poly(olefin sulfone)s **POSs 1–7** were designed to wrap pristine, unfunctionalized SWCNTs in solution to create isolated thin film networks. In addition to simple wrapping of SWCNTs with **POSs 1–7** (Figure 2; Approach A), poly(allyl alcohol sulfone) (**POS 8**), poly(2-allyl hexafluoroisopropanol sulfone) (**POS 9**), and poly(allylamine hydrochloride sulfone) (**POS 10**), were designed to display supramolecular interactions with noncovalently and covalently prefunctionalized SWCNTs (Figure 2; Approaches B–D).

Using **POS 8** or **9** as hydrogen bonding donor polymers, dispersions of SWCNTs prewrapped with **POS 4** (Approach B) and dispersions of covalently pyridyl-functionalized SWCNTs (*f*-**SWCNTs**)(Approach D) were complexed and shown to display additional stability. In addition to the stabilization of SWCNTs via noncovalent hydrogen-bonding and hydrophobic interactions, we further explored electrostatic interactions in the wrapping of SWCNTs (Approach C). In this layer-by-layer self-assembly approach, pristine SWCNTs were first noncovalently prefunctionalized in dispersion with pyrene tetrasulfonate (*pyr*). (31,32) In a second step, the polyanionic **SWCNTs-*pyr***dispersions were further stabilized by irreversible assembly with **POS 10** via Coulombic and entropic driven assembly.(31,32) In these assemblies, the aromatic core serves as an anchor to the sidewalls of the SWCNTs via π–π-stacking interactions to increase the water dispersibility of the system. Noncovalent functionalization procedures are less disruptive to the SWCNT electronic structure as compared to a covalent surface functionalization and thereby are expected to have higher intrananotube carrier mobilities.

Poly(olefin sulfone)s **POS 1–10** were characterized using standard techniques, including ^{1}H and ^{13}C NMR spectroscopy, gel-permeation chromatography (GPC), Fourier-transform infrared spectroscopy (FT-IR), dynamic light scattering (DLS), and thermogravimetric analysis (TGA). The molecular weights of all polymers were found to range between 17 and

173 kDa with dispersities (*D*) of 1.9–2.5. Table 1 displays the molecular weight data and decomposition temperatures of all poly(olefin sulfone)s investigated in this work. A successful noncovalent functionalization of SWCNTs using pyrene tetrasulfonate was proven by UV–vis-NIR absorption spectroscopy (see Supporting Information). The covalent attachment of pyridyl-units to the SWCNT sidewalls was accomplished by means of in situ diazonium chemistry (see SI).(31,32) This fast and simple functionalization sequence yielded *f*-**SWCNTs** which was evidenced by Raman microscopy, UV–vis-NIR spectroscopy, as well as X-ray photoelectron spectroscopy (XPS) (see Supporting Information). The analysis of the D-band intensity relative to the G-band intensity in the Raman spectra provided further evidence of successful covalent surface functionalization.

Characterization of POS-SWCNT Dispersions

UV–vis-NIR measurements provided insight into the SWCNT dispersion efficiencies of the synthesized polymers using the different coating Approaches A–D. The potential of the **POSs 1**–**10** to solubilize carbon nanotubes was determined by sonicating 0.1 wt% SWCNT-dispersions in the presence of an excess of POS (10 wt equiv) for 1 h at room temperature, followed by centrifugation (14,000 rpm) to remove large particulates that were not efficiently solubilized. The ratio of the absorbance of the coated SWCNTs at λ ~ 1000 nm (targeting the absorption of the 6,5-SWCNT majority species(33)) before and after centrifugation (Figure 3) represents the dispersion efficiency (Table 1).(34)

As the performance of the radiation sensor devices directly depends on the individualization of the individual SWCNTs in the POS-SWCNT composite active layer, the generation of the stable SWCNT dispersions is crucial. Not surprisingly, aliphatic **POSs 1** and **2** did not show pronounced interactions with the SWCNTs. The UV–vis-NIR spectra before and after centrifugation of a solution of 6,5-SWCNTs and **POS 1** in DMF are displayed in Figure 3a (Entry #1). Alternatively, **POSs 3** and **4** resulted in an increased dispersion efficiency of 4.7% and 7.2%. The isolated supernatant from the centrifuged suspensions contained well-dispersed POS-SWCNT composites that resisted rebundling and aggregation over extended periods (>5 days). In addition to the dispersion efficiency, confirmation of SWCNT individualization is necessary to evaluate the quality of the dispersions. Figure 3b displays normalized absorbance spectra of a **POS 4**-SWCNT dispersion before and after centrifugation. The peaks, arising from the SWCNT optical transitions were significantly sharper and more intense relative to the base absorbance background upon which the spectra are normalized. Amphiphilic **POSs 5** and **6** showed the most stable dispersions of 26.6% and 31.3%, respectively. This was attributed to a solubilizing effect of the polar polymer side chains and the hydrophobically enhanced van der Waals association between the alkyl moieties and the CNT surfaces. Beyond providing information about the dispersion efficiency and individualization, the absorbance spectra of **POS 9**-*f*-SWCNT (Table 1; Entry #15) demonstrated a further evidence for a successful covalent surface functionalization. Individualized pristine SWCNT samples typically show pronounced optical transitions, arising from the van Hove singularities. These features are reduced by the covalent attachment of pyridyl-group and the well-dispersed supernatant in DMF of entry 15 was characterized by a reduction of defined interband transitions (Figure 3a).

Resistive γ-Ray Dosimeters

Sensors using POS-SWCNT composites were fabricated by spray-coating POS-SWCNT dispersions onto glass substrates. A shadow mask was used to selectively deposit POS-SWCNT dispersions between Au electrodes separated by 1.0 mm. The glass-electrode substrates were heated on a hot plate at 90 °C for rapid solvent evaporation and to quickly pin the SWCNTs in random individualized networks. The spray-coating was adjusted such that the deposited POS-SWCNT had a resistance of $R_0 \sim 10$ kΩ as measured by a multimeter. Sensor testing was performed using a Gammacell irradiator with a ^{60}Co source. By connecting the resistive device via wires to a digital multimeter, real-time dosimetric read-outs with γ-ray irradiation were observed (Figure 4a).

To compare the maximum performance of the different composites, the devices were exposed to 40 krad. The resistance of all well-dispersed POS-SWCNT composites rapidly decreased exponentially until saturation was reached. As expected, composites with poor SWCNT dispersion prepared with **POS 1** or **2** showed little response to gamma irradiation. In general, the dispersion efficiencies correlate well with the response of the POS-SWCNT composites to γ-radiation (Figure 4b). Other factors, including the solvent, the intrinsic POS stability, as well as the type of SWCNT (pristine vs functionalized) also influence the device performance. In devices prepared with amphiphilic **POSs 5** and **6**, that were spray-coated from an aqueous solution, we observed a rapid onset of the resistance decrease. In control devices prepared from polymer-free SWCNT dispersions we observed slight resistance increases at 40 krad, whereas all other devices from POS-SWCNT composites (entries #3–15) resulted in resistance decreases. Composite 15 (**POS 9**and *f*-SWCNTs) displayed the highest response to γ-rays with a resistance decrease $R = R'/R_0 \times 100$ of up to −65% at 40 krad.

Influence of Bismuth Components

The γ-ray opacity of materials increases with increasing Z(atomic number). Therefore, we anticipated that integration of high atomic number elements into the polymer matrix would result in a concomitant increase the γ-ray cross-section values of the active layer and lead to a higher device sensitivity. As an alternative to a tedious functionalization of POSs with a soluble bismuth complex, as has been done for **POS 7**, we targeted Bi nanoparticles (Bi-NP) as additional components for our polymer matrices. Dodecanethiol-functionalized Bi-NPs were synthesized according to a literature method.(35) To ensure uniform dispersions with our lead composition, Entry 15, the Bi-NPs were then treated with **POS 5** to form core–shell structures as outlined in Figure 5. The addition of Bi-NPs to the POS-SWCNT composite provides some resistance decrease R relative to similar thickness metal-free films; however, the sensitivity of the devices increases significantly with this addition. The Bi-NP augmented version of Entry 15 showed a 50% greater resistance loss at a γ-ray dose of 5 krad. This simple admixing of high atomic number NP components represents a facile and pragmatic approach for the generation of POS-SWCNT composite materials with a high opacity toward γ-ray irradiation with greatly minimized synthetic effort.

Capacitive γ-Ray Dosimeters

Encouraged by the performance of the POS–SWCNT composites as resistive γ-ray dosimeters, we explored their performance in a commercial capacitive platform.(36) Here, the polymer-CNT composite functions as a dielectric material in a miniaturized capacitive sensor equipped with three individual parallel-plate sensing capacitors with a fixed gap (0.75 μm). The devices were coated by drop-casting the POS-SWCNT dispersions onto the sensor platform.

In contrast to resistive devices, in capacitive sensors the SWCNTs need not be transformed into a state with macroscopic conductivity. The circuit operates by measuring the electrode charging that occurs when the sensor bias is switched to drive the sensor capacitor between charging and discharging (Figure 6).(36) The sensor bias was switched using a square-wave voltage pulse at a kilohertz frequency. As the capacitance strongly depends on the dielectric constant, base values were obtained for the pure polymers, without SWCNTs. Figure 6 displays the real-time performance of selected POS-CNT composites in capacitive sensors.

The signal-to-noise ratio of devices coated with pure POSs was low and obstructed clear dosimetric determination of irradiation results. Devices coated with POS-SWCNT composites resulted in significantly higher signal-to-noise ratios that closely correlated with the dispersion efficiency. As a result, a smooth increase of the capacitance signal $C = C'/C_0$ was observed for the devices coated with the most stable composites 6, 7, and 15. In agreement with the resistive performance of POS-SWCNT Entry 15 (**POS 9** and *f*-SWCNTs), this composite also most sensitively responded to a γ-irradiation in the capacitive devices, resulting in a maximum response of $C = +40\%$ at radiation doses of >40 krad. The ease of fabrication and low power consumption of these small and inexpensive sensor platforms combined with the highly appealing sensitivity parameters of the newly synthesized polymer matrices further demonstrates the potential of poly(olefin sulfone)-SWCNT composites to serve as a new transduction materials in γ-ray dosimeters.

Conclusion

In summary, we describe new advanced POS-SWCNT composite materials as transduction materials for γ-ray dosimeters. Metastable poly (olefin sulfone)s readily depolymerize when exposed to ionizing radiation, and were designed to strongly interact with both nonfunctionalized and functionalized SWCNTs. The polymer-SWCNT composites were readily deposited as active layers in resistive and capacitive γ-ray dosimeters. The use of Bi-NPs also increases the sensitivity by increasing the γ-ray opacity. The use of a radiation sensitive carbon nanotube based electronic circuits to provide a signal gain represents a powerful, straightforward, and inexpensive approach to real-time radiation dosimeters.

Supplementary Material

Refer to Web version on PubMed Central for supplementary material.

References

1. Knoll GF Radiation detection and measurement, 4th ed; John Wiley & Sons: Hoboken, 2010.

2. Kulp WD In Energy Nuclear, N. Tsoulfanidis, Ed.; Springer: New York, 2013; pp 427– 444.

3. Del Sordo S; Abbene L; Caroli E; Mancini AM; Zappettini A; Ubertini P Progress in the development of CdTe and CdZnTe semiconductor radiation detectors for astrophysical and medical applications. Sensors 2009, 9, 3491–3526, DOI: 10.3390/s90503491 [PubMed: 22412323]

4. Pushpavanam K; Narayanan E; Rege K Molecular and Nanoscale Sensors for Detecting Ionizing Radiation in Radiotherapy. ChemNanoMat 2016, 2, 385–395, DOI: 10.1002/cnma.201600064

5. Ma J; Yeow JT; Chow JC; Barnett R A carbon nanotube-based radiation sensor. International Journal of Robotics & Automation 2007, 22, 49–58, DOI: 10.2316/Journal.206.2007.1.206-1005

6. Yu L; Shearer C; Shapter J Recent development of carbon nanotube transparent conductive films. Chem. Rev 2016, 116, 13413–13453, DOI: 10.1021/acs.chemrev.6b00179 [PubMed: 27704787]

7. Dong X; Hu F; Liu Z; Zhang G; Zhang D A fluorescent turn-on low dose detection of gamma-radiation based on aggregation-induced emission. Chem. Commun 2015, 51, 3892–3895, DOI: 10.1039/C4CC10133B

8. Benevides CA; de Menezes FD; de Araujo RE Evaluation of fluorescent dye degradation indirectly induced by x-ray ionizing radiation. Appl. Opt 2015, 54, 6935–6939, DOI: 10.1364/AO.54.006935 [PubMed: 26368112]

9. Arregui FJ Sensors based on nanostructured materials; Springer: New York, 2009.

10. Esser-Kahn AP; Sottos NR; White SR; Moore JS Programmable microcapsules from self-immolative polymers. J. Am. Chem. Soc 2010, 132, 10266–10268, DOI: 10.1021/ja104812p [PubMed: 20662509]

11. Peterson GI; Larsen MB; Boydston AJ Controlled depolymerization: stimuli-responsive self-immolative polymers. Macromolecules 2012, 45, 7317–7328, DOI: 10.1021/ma300817v

12. Roth ME; Green O; Gnaim S; Shabat D Dendritic, oligomeric, and polymeric self-immolative molecular amplification. Chem. Rev 2016, 116, 1309–1352, DOI: 10.1021/acs.chemrev.5b00372 [PubMed: 26355446]

13. Fan B; Trant JF; Wong AD; Gillies ER Polyglyoxylates: a versatile class of triggerable self-immolative polymers from readily accessible monomers. J. Am. Chem. Soc 2014, 136, 10116–10123, DOI: 10.1021/ja504727u [PubMed: 24956012]

14. Kaitz JA; Diesendruck CE; Moore JS End group characterization of poly (phthalaldehyde): surprising discovery of a reversible, cationic macrocyclization mechanism. J. Am. Chem. Soc 2013, 135, 12755–12761, DOI: 10.1021/ja405628g [PubMed: 23924340]

15. Cai K; Yen J; Yin Q; Liu Y; Song Z; Lezmi S; Zhang Y; Yang X; Helferich WG; Cheng J Redox-responsive self-assembled chain-shattering polymeric therapeutics. Biomater. Sci 2015, 3, 1061–1065, DOI: 10.1039/C4BM00452C [PubMed: 26146551]

16. Ishihara S; Azzarelli JM; Krikorian M; Swager TM Ultratrace detection of toxic chemicals: triggered disassembly of supramolecular nanotube wrappers. J. Am. Chem. Soc 2016, 138, 8221–8227, DOI: 10.1021/jacs.6b03869 [PubMed: 27336905]

17. Gnaim S; Shabat D Quinone-methide species, a gateway to functional molecular systems: from self-immolative dendrimers to long-wavelength fluorescent dyes. Acc. Chem. Res 2014, 47, 2970–2984, DOI: 10.1021/ar500179y [PubMed: 25181456]

18. Lee OP; Lopez Hernandez H; Moore JS Tunable Thermal Degradation of Poly (vinyl butyl carbonate sulfone) via Side-Chain Branching. ACS Macro Lett. 2015, 4, 665–668, DOI: 10.1021/acsmacrolett.5b00234

19. Sasaki T; Hashimoto S; Nogami N; Sugiyama Y; Mori M; Naka Y; Le KV Dismantable Thermosetting Adhesives Composed of a Cross-Linkable Poly(olefin sulfone) with a Photobase Generator. ACS Appl. Mater. Interfaces 2016, 8, 5580–5585, DOI: 10.1021/acsami.5b10110 [PubMed: 26872271]

20. Possanza Casey CM; Moore JS Base-Triggered Degradation of Poly(vinyl ester sulfone)s with Tunable Sensitivity. ACS Macro Lett. 2016, 5, 1257–1260, DOI: 10.1021/acsmacrolett.6b00698

21. Brown J; O'Donnell J γ Radiolysis of poly(butene-1 sulfone) and poly (hexene-1 sulfone). Macromolecules 1972, 5, 109–114, DOI: 10.1021/ma60026a001

22. Bowmer TN; O'Donnell JH Radiation degradation of poly (olefin sulfone)s: a volatile product study. J. Macromol. Sci., Chem 1982, 17, 243–263, DOI: 10.1080/00222338208063258

23. Orellana G; Moreno-Bondi MC Frontiers in chemical sensors: novel principles and techniques; Springer:Heidelberg, 2006.

24. Fennell JF; Liu SF; Azzarelli JM; Weis JG; Rochat S; Mirica KA; Ravnsbaek JB; Swager TM Nanowire chemical/biological sensors: Status and a roadmap for the future. Angew. Chem., Int. Ed 2016, 55, 1266–1281, DOI: 10.1002/anie.201505308

25. Aida T; Meijer E; Stupp S Functional supramolecular polymers. Science 2012, 335, 813–817, DOI: 10.1126/science.1205962 [PubMed: 22344437]

26. Whittell GR; Hager MD; Schubert US; Manners I Functional soft materials from metallopolymers and metallosupramolecular polymers. Nat. Mater 2011, 10, 176–188, DOI: 10.1038/nmat2966 [PubMed: 21336298]

27. Tsouti V; Boutopoulos C; Zergioti I; Chatzandroulis S Capacitive microsystems for biological sensing. Biosens. Bioelectron 2011, 27, 1–11, DOI: 10.1016/j.bios.2011.05.047 [PubMed: 21752630]

28. Lobez JM; Swager TM Radiation detection: Resistivity responses in functional poly (olefin sulfone)/carbon nanotube composites. Angew. Chem., Int. Ed 2010, 49, 95–98, DOI: 10.1002/anie. 200904936

29. Yoon B; Liu SF; Swager TM Surface-Anchored Poly (4-vinylpyridine)–Single-Walled Carbon Nanotube–Metal Composites for Gas Detection. Chem. Mater 2016, 28, 5916–5924, DOI: 10.1021/acs.chemmater.6b02453

30. Rouse JH Polymer-assisted dispersion of single-walled carbon nanotubes in alcohols and applicability toward carbon nanotube/sol-gel composite formation. Langmuir 2005, 21, 1055–1061, DOI: 10.1021/la0481039 [PubMed: 15667189]

31. Savagatrup S; Schroeder V; He X; Lin S; He M; Yassine O; Salama KN; Zhang XX; Swager TM Bio-Inspired Carbon Monoxide Sensors with Voltage-Activated Sensitivity. Angew. Chem., Int. Ed 2017, 56, 14066–14070, DOI: 10.1002/anie.201707491

32. Bosch S; Zeininger L; Hauke F; Hirsch A A Supramolecular Approach for the Facile Solubilization and Separation of Covalently Functionalized Single-Walled Carbon Nanotubes. Chem. - Eur. J 2014, 20, 2537–2541, DOI: 10.1002/chem.201303506 [PubMed: 24481923]

33. Tu X; Manohar S; Jagota A; Zheng M DNA sequence motifs for structure-specific recognition and separation of carbon nanotubes. Nature 2009, 460, 250–253, DOI: 10.1038/nature08116 [PubMed: 19587767]

34. Coleman JN Liquid-phase exfoliation of nanotubes and graphene. Adv. Funct. Mater 2009, 19, 3680–3695, DOI: 10.1002/adfm.200901640

35. Son JS; Park K; Han MK; Kang C; Park SG; Kim JH; Kim W; Kim SJ; Hyeon T Large-scale synthesis and characterization of the size-dependent thermoelectric properties of uniformly sized bismuth nanocrystals. Angew. Chem., Int. Ed 2011, 50, 1363–1366, DOI: 10.1002/anie.201005023

36. Mlsna TE; Cemalovic S; Warburton M; Hobson ST; Mlsna DA; Patel SV Chemicapacitive microsensors for chemical warfare agent and toxic industrial chemical detection. Sens. Actuators, B 2006, 116, 192–201, DOI: 10.1016/j.snb.2005.12.066
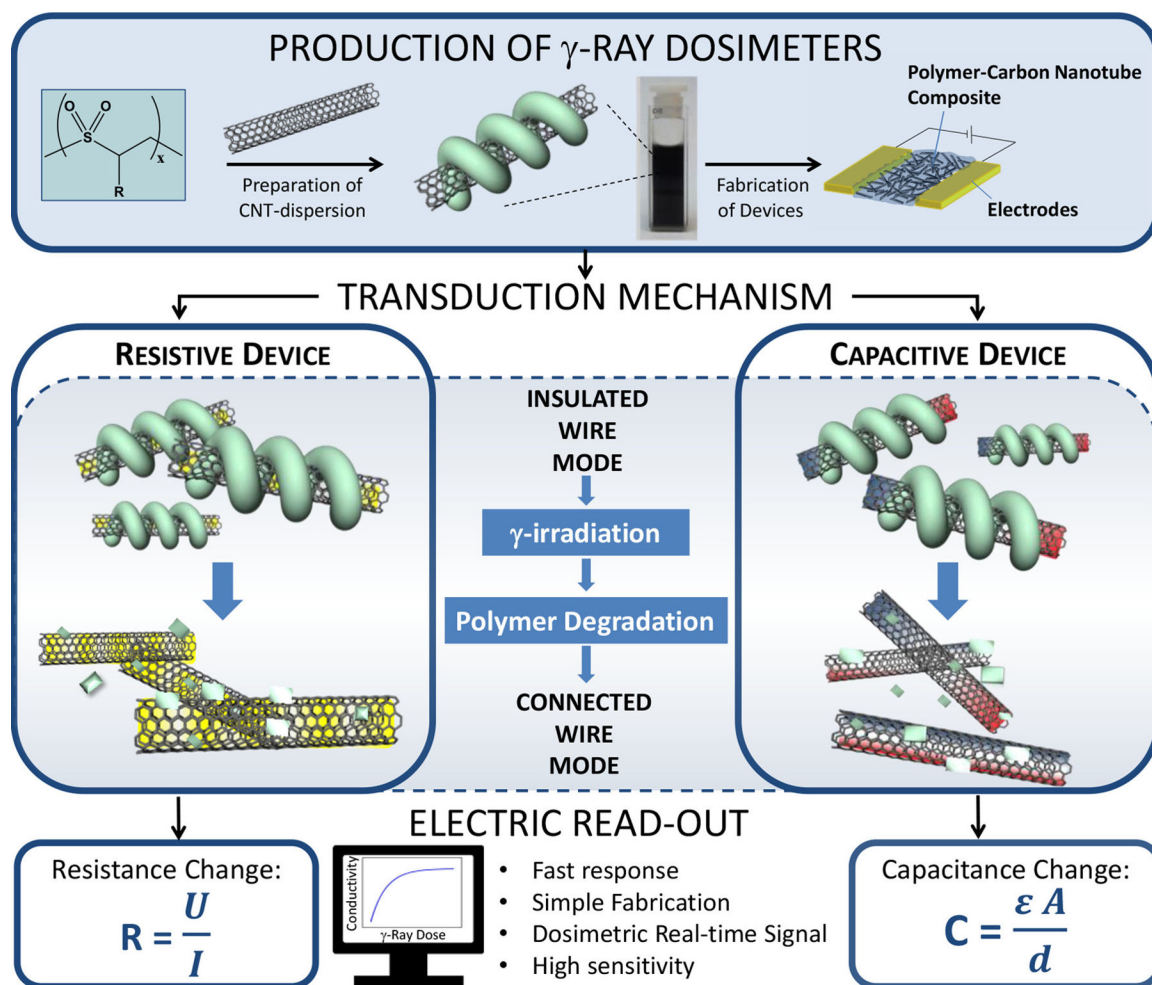
Scheme 1.
Illustration of the Dispersion of SWCNTs by Wrapping with POS Chains (top) and How γ-Ray Initiated Depolymerization of the POS Can Create Resistive or Capacitive Responses (bottom)
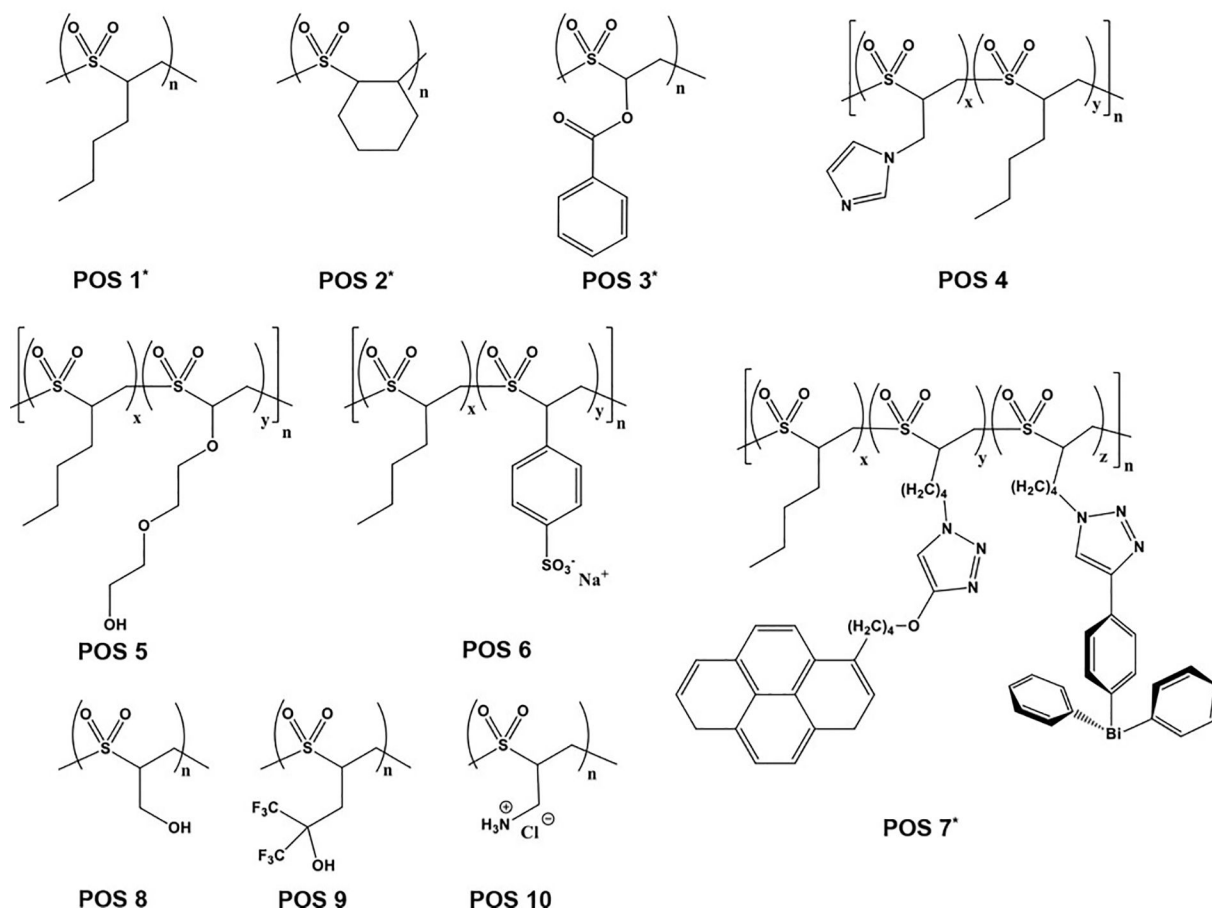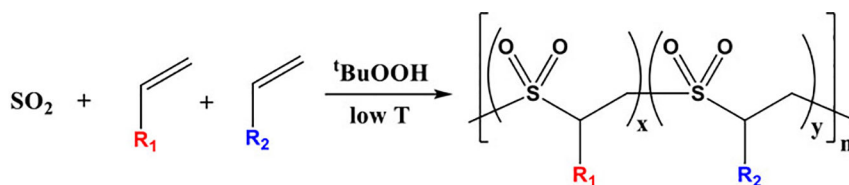
Figure 1.
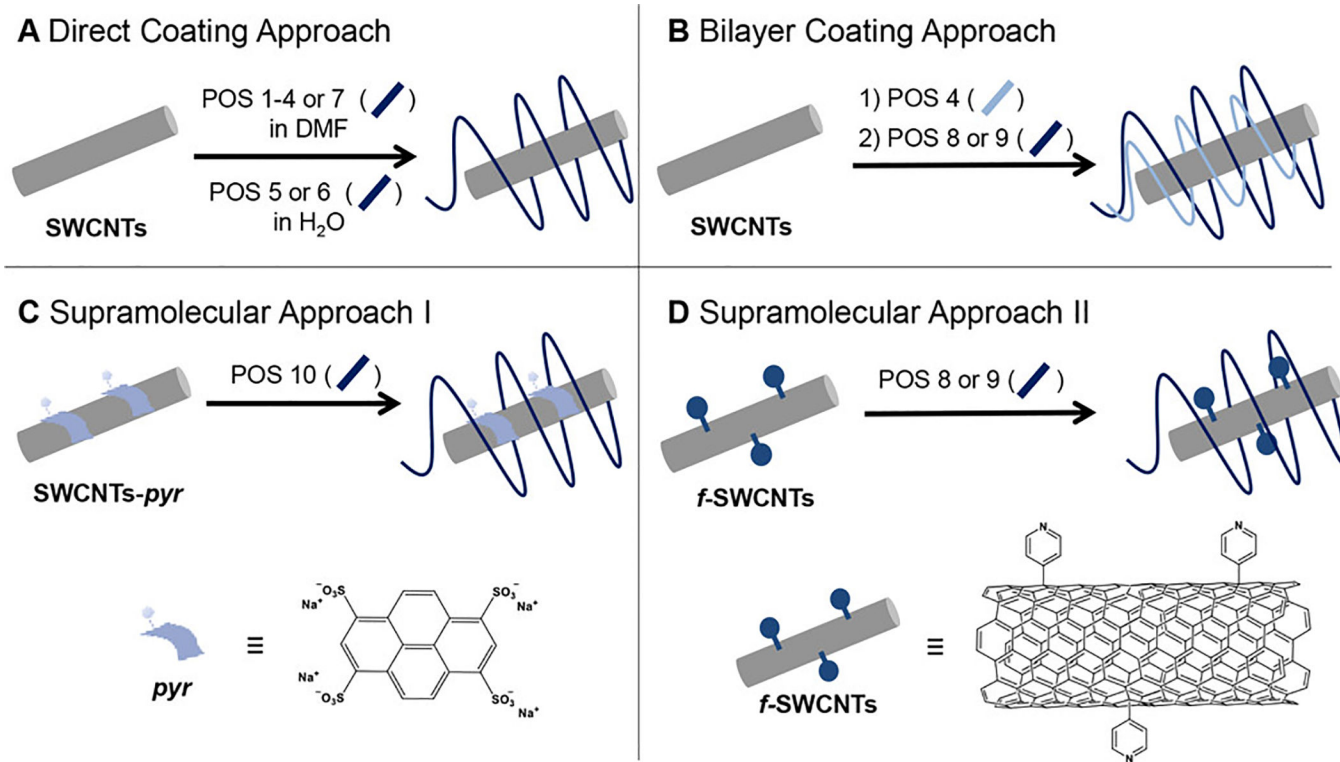Synthesis and structures of new and previously reported (*) poly(olefin sulfone)s prepared for this study.

Figure 2.
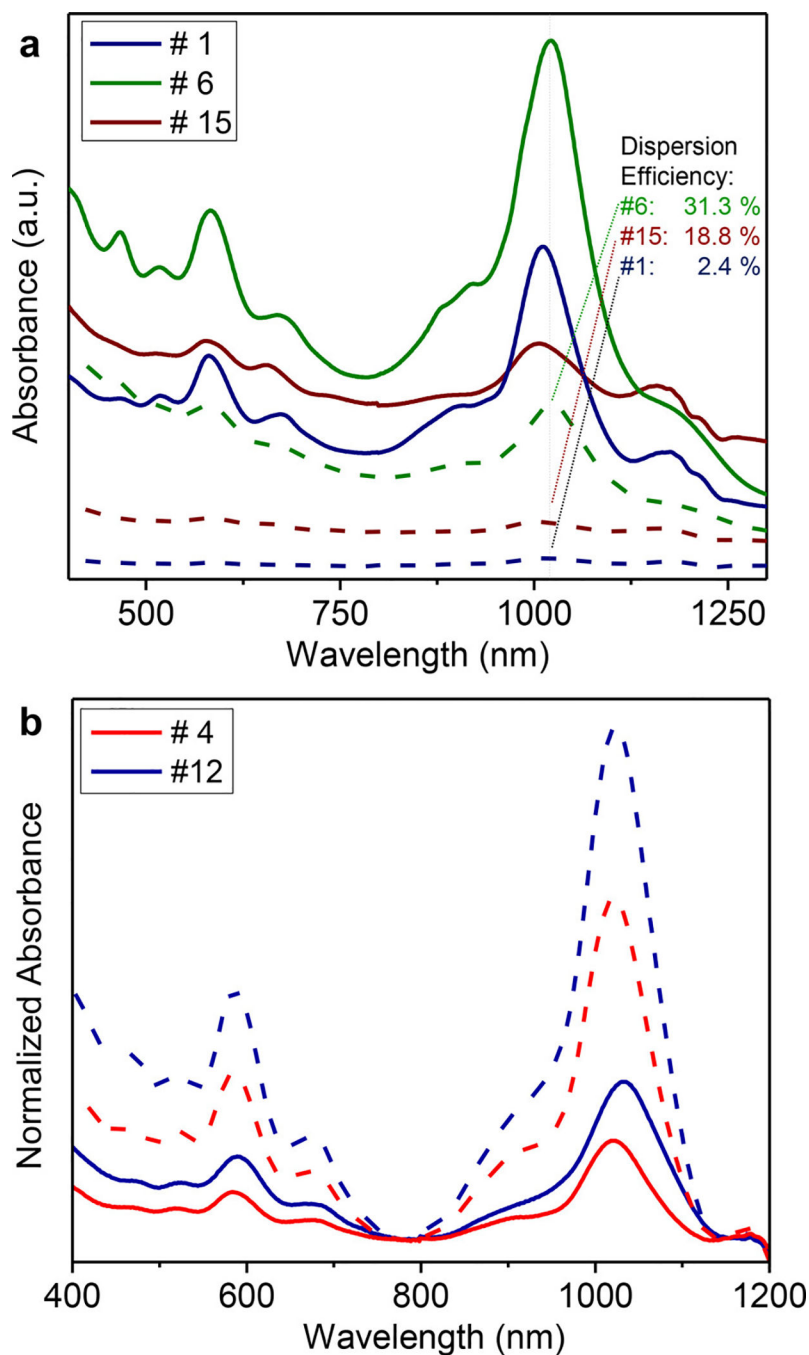Four wrapping approaches investigated in this study for SWCNTs using **POSs 1–10**.

Figure 3.
UV–vis-NIR spectra of selected POS-SWCNT dispersions. Absorption spectra of SWCNTs dispersed in POS-DMF solution before (dashed lines) and after (solid lines) centrifugation. After centrifugation, the sample is mainly composed of individualized SWCNTs, but at a lower concentration: (a) the dispersion efficiency in % is calculated by taking the ratio of the absorbance of the supernatant before and after centrifugation; (b) the degree of debundling is indicated by the relative intensity of the normalized absorbance spectra.
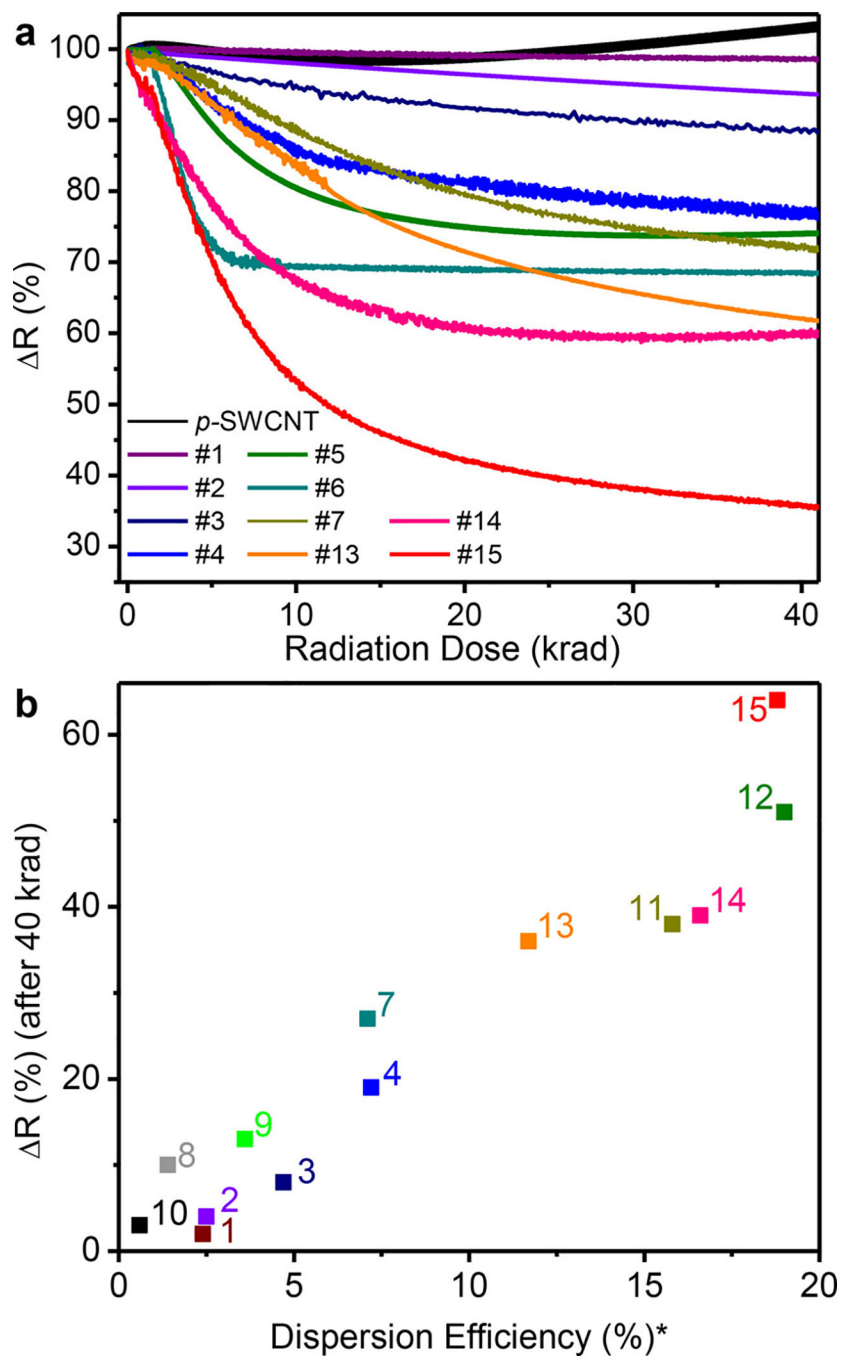
Figure 4.
(a) Real-time resistance changes of selected POS-CNT nanocomposites during γ-ray irradiation (see Table 1 for POS-SWCNT composites #1–#15); (b) Sensitivity to γ-rays of SWCNT-POS composites deposited from DMF as a function of the dispersion efficiency (*Calculation of the dispersion efficiency is detailed in the text).
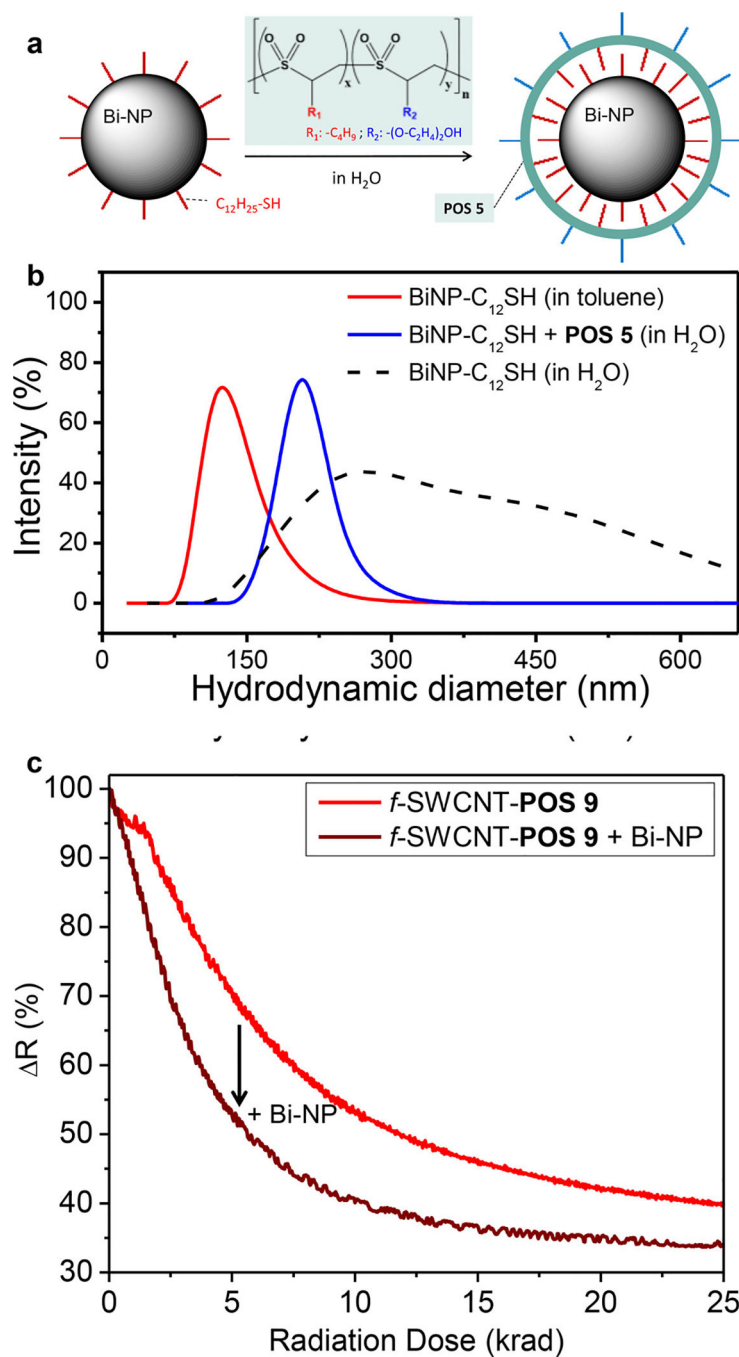
Figure 5.
(a) Wrapping of Bi-NPs with amphiphilic **POS 5**. (b) DLS curves demonstrating the stabilization of Bi-NPs in polar solutions by **POS 5**. (c) Device performance before and after addition of **POS 5**-coated Bi-NPs to composite #15 (**POS 9** and *f*-SWCNTs).
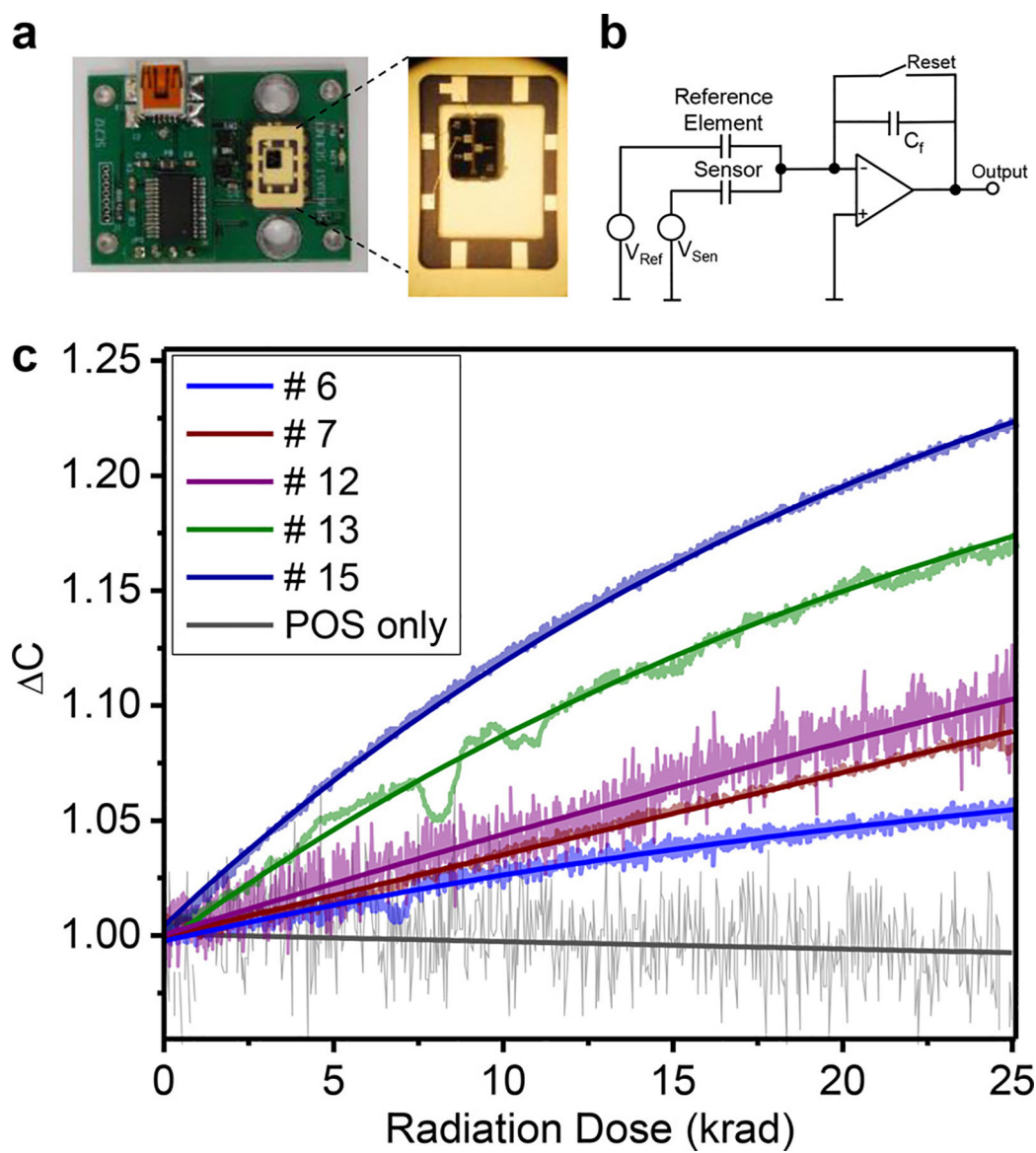
Figure 6.
(a) Image of the capacitive sensor board with sensor chip. (b) Scheme of the electric circuit.
(c) Real-time performance of selected POS-CNT nanocomposites to γ-radiation in the
capacitive devices: original signals and exponential fits.

Table 1.

Characterization of Synthesized Polymers POS 1–10 and Their CNT Dispersion Efficiencies

entry	polymer synthesis and characterization					SWCNT dispersion		
#	polymer(s)	yield (%)	M_n	D	T_{decomp}(°C)	CNT	wrapping approach[a]	solvent	disp. eff.[b] (%)
1	POS 1	98	84	2.3	246	SWCNT	A	DMF	2.4
2	POS 2	76	26	2.2	232	SWCNT	A	DMF	2.5
3	POS 3	61	S3	2.2	188	SWCNT	A	DMF	4.7
4	POS 4	78	60	2.3	148	SWCNT	A	DMF	7.2
5	POS 5	59	49	2.5	156	SWCNT	A	H_2O	26.6
6	POS 6	75	44	2.2	262	SWCNT	A	H_2O	31.3
7	POS 7	-	17	2.1	197	SWCNT	A	DMF	7.1
8	POS 8	66	35	1.9	273	SWCNT	A	DMF	1.4
9	POS 9	91	173	2.0	281	SWCNT	A	DMF	3.6
10	POS 10	86	37	1.9	182	SWCNT	A	H_2O	0.6
11	POSs 4 and 8	-	-	-	-	SWCNT	B	DMF	15.8
12	POSs 4 and 9	-	-	-	-	SWCNT	B	DMF	19.0
13	POS 10	86	37	1.9	182	SWCNT-*pyr*	C	H_2O	11.7
14	POS 8	66	35	1.9	273	*f*-SWCNT	D	DMF	16.6
15	POS 9	91	173	2.0	281	*f*-SWCNT	D	DMF	18.8

[a]As outlined in Figure 2.

[b]Caclulation of the dispersion effciency is detailed in the text.